Analysis of SPM Servo Motor with Static, Dynamic and Mixed Eccentricity in Aspects of Vibration and Noise

Shaofeng Jia, Student Member, IEEE, Ronghai Qu*, Senior Member, IEEE, Jian Li, Senior Member, IEEE, Zansong Fu, Leilei Wu, Hong Chen
State Key Laboratory of Advanced Electromagnetic Engineering and Technology
Huazhong University of Science and Technology
*:ronghaiqu@mail.hust.edu.cn

***Abstract*—This paper discusses the effect of eccentricity, including static, dynamic and mixed eccentricity on the performance of SPM servo motor. The electromagnetic performance such as back-EMF, torque quality, unbalanced magnetic pull (UMP) under different kinds of eccentricity are investigated and compared using finite element analysis (FEA). With the electromagnetic radial force obtained from electro-magnetic FEA, we predict the vibration of the stator housing, and acoustic noise around the machine. The results of this study show that the eccentricity has little effect on the back-EMF, but the cogging torque, torque ripple, vibration and noise are dramatically increased when the rotor eccentricity occures, especially under load condition. The analysis results are verified by experiment and good agreement has been achieved. The conclusin of this study is instructive for the development of electric motors which are used in servo drive system and other similar applications.**

***Keywords*—Cogging torque, Eccentricity, SPM, Torque Ripple, UMP, Vibration and Noise**

I. INTRODUCTION

For servo motors used in numerical control machine tool drive system, vibration is one of the most important performance characteristics to be considered in the design process [1]. Nowadays, Permanent Magnet Synchronous Motor is widely used in servo drive system due to their features of high power density, better dynamic performance, simple construction, easy maintenance and especially the characteristic of low vibration and noise. Design choice of high-power density requires a relatively small air gap which puts forward a very high request to the manufacture and assembly process in order to insure the air-gap uniform. Due to the fabrication tolerances, a relative eccentricity between the stator and rotor of nearly 10% is common [2].

Eccentricity can occur due to many reasons such as poor dynamic balance of rotor, the abrasion of bearings after long-running, the shaft being bending, the structure deformation and fabrication tolerances aforementioned. Generally speaking, Eccentricity can be divided into the following three basic types which are static eccentricity (SE), dynamic eccentricity (DE), and mixed eccentricity (ME). So far, many existing literatures have done two aspects research about eccentricity. One is focus on the effects of static and dynamic eccentricity on electromagnetic performance, the other is primarily on the detection of eccentricity online and offline. In [4], the author comprehensively investigates the electromagnetic performance of permanent magnet machines having static or dynamic eccentricity such as flux density, back-EMF and electromagnetic torque with different slot/pole number combination and winding configuration. It shows that for symmetrical machines, eccentricity does not affect the back-EMF and torque, but for asymmetric machines, it significantly distorts the back-EMF and torque. In [5], the paper discusses the erect of the degree of DE on the cogging torque of PM generators for small wind turbines, the conclusion is helpful to design a PM generator that starts-up at a low wind speed. In [], the eccentricity of conventional induction machine and PM machine have been diagnosed and detected online or offline mainly based on the induced specific harmonics induced in the stator current spectrum or the change of the inductance. In [6], the eccentricity type can be identified by a k-NN classifier and their eccentricity severity can be estimated by MLP neural networks. The concept of k-NN classifier and MLP neural networks is first introduced in [7] and [8].

Although the operation of PM machines is the quietest compared to other conventional machines such as induction and switched reluctance machines, the vibration and acoustic noise are still serious issues when applied in servo system, consumer products, etc [9]. Generally speaking, noise and vibration may originate from electromagnetic, mechanical, and aerodynamic sources, but the electromagnetically induced noise is the dominant for small-power machines [9]. To the research of the vibration of PM machines, many scholars have done a lot of meaningful

978-1-4799-5776-7/14/$31.00

work. Paper [9] proposes an analytical method to evaluate the electromagnetic vibration and acoustic noise of both radial and axial flux surface mounted PM machines in order to design and optimize a low noise motor. Paper [11] systematically investigates the influence of slot and pole number combination including the frequent used combination such as $2p = N_s \pm 2, 2p = N_s \pm 1, q = 0.5$ on the radial force and vibration modes in fractional slot PM machines having single- and double-layer windings, the conclusion is helpful to select the slot and pole combination in designing a low vibration machine. In [12], it studies the influence of the stator slotting and the circumferential air-gap field component on the radial force in PM machines with load, and the analytical results show that this influence can be ignored when investigating the radial force which is critical for the machine vibration. Besides, according to many literatures published, radial force, tangential force, and torque ripple are the main excitation sources to generate the electromagnetic vibration while the radial force is the most important one among the three for vibration analysis. Also, some paper investigate and compare the effect of the winding type of FSCW and ISDW and the rotor type of IPM and SPM on vibration and draw the conclusion that in general, the vibration of IPM machine is higher than SPM due to larger armature reaction and FSCW is larger than ISDW as a result of richer harmonics and lower dominant vibration mode usually as 1or 2.

The electromagnetic induced vibration can be caused by radial force, unbalanced magnetic pull (UMP), torque ripple. Generally, the radial force and UMP have large effect on vibration. A machine with eccentricity will have non uniform air-gap which will distort the radial force and UMP and change the vibration and noise level. Hence, the aim of this paper is to investigate and compare the effect of eccentricity type on PM machine performance. The main work of this paper is as follows:

First, an SPM motor with SE, DE and ME is modeled and analyzed using time-stepping finite element analysis (TSFEA), respectively. Second, the electromagnetic performance such as back-EMF, cogging torque, torque and torque ripple, UMP are investigated and compared. The results show that the cogging torque and torque ripple will heavily increase with eccentricity which will dramatically degrade the system performance. Besides, the vibration and noise are predicted and compared with the health motor. The results show that the vibration with eccentricity will increase than the health condition for easier resonance in some specific harmonic electromagnetic force. Perfect agreement have been achieved between the experiment results and FEA analysis.

II. FEM MODEL OF SERVO MOTOR AND ECCENTRICITY DEFINITION

A. Machine Specifications

A schematic of a radial flux SPM motor which is used as a servo motor is shown in Fig.1. The parameters of the machine are given in Table I.

B. Eccentricity Definition

Fig.2 shows the three types of eccentricity. SE (Fig.2a), DE (Fig.2b), ME (Fig.2c), and health machine (Fig.2d). The health machine is used to make comparison.

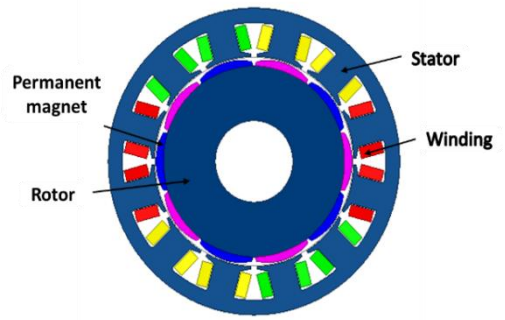

Fig.1 Construction of a SPM servo motor

TABLE I. MAIN PARAMETERS OF THE SPM MOTOR

Parameter	Values
Number of poles	10
Stator slots	12
Stator Outer diameter(mm)	125
Stator Inner diameter(mm)	86
Air-gap length(mm)	0.8
Rotor Inner diameter(mm)	84.4
Turns per slot	42
Stack length(mm)	36
Remanent flux density of PM (T)	1.203
Rated frequency(Hz)	125

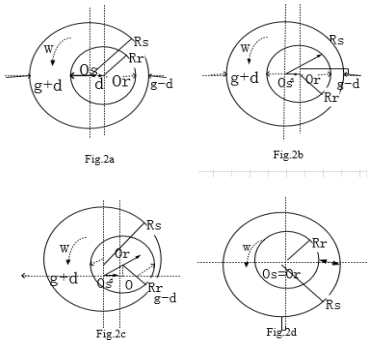

Fig.2 Motor eccentricity: a) static; b) dynamic; c) mixed; d) health.

C. Air-gap length with eccentricity

The air-gap length is a key design parameter for machine performance because of the low permeability of air. The air-gap length with various eccentricity is defined as follows:

SE: $$g_s = g \cdot k_s \quad (1)$$

k_s is the modulation effect of SE on air-gap length and is defined as:

$$k_s = 1 + \delta_s \cos(\theta - \theta_s) \quad (2)$$

DE: $$g_d = g \cdot k_d \quad (3)$$

k_d is the modulation effect of DE on air-gap length and is defined as:

$$k_d = 1 + \delta_d \cos(\omega_r t - (\theta - \theta_d)) \quad (4)$$

ME:

$$g_m = g \cdot k_m \quad (5)$$

k_m is the modulation effect of ME on air-gap length and is defined as:

$$k_m = 1 + \delta_s \cos(\theta - \theta_s) + \delta_d \cos(\omega_r t - (\theta - \theta_d)) \quad (6)$$

where g is the designed air-gap length, δ_s is the SE degree, θ is the mechanical rotor position, θ_s is the initial position of SE which the air-gap length is maximal, δ_d is the DE degree, ω_r is the mechanical angular velocity, t is time, θ_d is the initial position of DE which the air-gap length is maximal.

In this paper, we analyze 0.5 degree eccentricity of SE, DE and ME. δ_s is 0.5 and δ_d is 0.5 in SE and DE, separately, while in ME, we set δ_s and δ_d both 0.25.

III. MAGNETIC FIELD ANALYSIS WITH ECCENTRICITY

Magnetic field contains full information of machine including the stator, rotor, and the other properties. In order to simplify the analysis, we ignore the saturation effect of the steel core, besides, neglect the circumferential airgap field component and consider the radial component only, thus, the analyses can be significantly simplified.

A. Magnet field analysis

Open-circuit magnet field of PM machines considering stator slotting effect had been analyzed in [13], the field of health machines can be expressed as:

$$\begin{aligned} B_{r\_mag} &= \sum_{k_1}^{1,3,5} B_{rmk_1} \cos[k_1 p(w_r t - \theta)] \times \sum_{k_2}^{0,1,2} \Lambda_{k_2} \cos(k_2 N_s \theta) \\ &= \sum_{k_1}^{1,3,5} \sum_{k_2}^{0,1,2} B_{rmk_1} \Lambda_{k_2} \cos[k_1 p w_r t - (k_1 p \pm k_2 N_s \theta)] \end{aligned} \quad (7)$$

where k_1 is the harmonic order, p is the number of pair, k_2 is the slot harmonic order, N_s is the number of stator slots, Λ_{k2} is the modulation effect of stator slotting on amplitude of magnetic field and can be found in [14].

When the eccentricity occurs, the airgap length will distort, the magnetic field can be thought of a modulation effect of un-uniform gap on the health field and can be summarized as follows:

With SE,

$$\begin{aligned} B_{s\_r\_mag} &= \frac{B_{r\_mag}}{k_s} \\ &= \frac{\sum_{k_1}^{1,3,5} \sum_{k_2}^{0,1,2} B_{rmk_1} \Lambda_{k_2} \cos[k_1 p w_r t - (k_1 p \pm k_2 N_s \theta)]}{1 + \delta_s \cos(\theta - \theta_s)} \end{aligned} \quad (8)$$

With DE,

$$\begin{aligned} B_{d\_r\_mag} &= \frac{B_{r\_mag}}{k_d} \\ &= \frac{\sum_{k_1}^{1,3,5} \sum_{k_2}^{0,1,2} B_{rmk_1} \Lambda_{k_2} \cos[k_1 p w_r t - (k_1 p \pm k_2 N_s \theta)]}{1 + \delta_d \cos(\omega_r t - (\theta - \theta_d))} \end{aligned} \quad (9)$$

With ME,

$$\begin{aligned} B_{m\_r\_mag} &= \frac{B_{r\_mag}}{k_m} \\ &= \frac{\sum_{k_1}^{1,3,5} \sum_{k_2}^{0,1,2} B_{rmk_1} \Lambda_{k_2} \cos[k_1 p w_r t - (k_1 p \pm k_2 N_s \theta)]}{1 + \delta_s \cos(\theta - \theta_s) + \delta_d \cos(\omega_r t - (\theta - \theta_d))} \end{aligned} \quad (10)$$

From the above theoretical analysis, we can get the open circuit air-gap flux density frequency order and spatial mode order as:

SE: $[k_1 p, [-k_1 p \pm k_2 N_s, -k_1 p \pm k_2 N_s \pm 1]]$,

DE: $[[k_1 p, k_1 p \pm 1], [k_1 p \pm k_2 N_s, k_1 p \pm k_2 N_s \pm 1]]$,

ME: $[[k_1 p, k_1 p \pm 1], [k_1 p \pm k_2 N_s, k_1 p \pm k_2 N_s \pm 1]]$

where $k_1 = 1,3,5,\cdots$, $k_2 = 0,1,2,\cdots$

For the 12 slots 10 poles machine, the corresponding frequency and spatial mode order is summarized in Tab. II.

TABLE II. MAGNET FIELD FREQUENCY AND MODE ORDER OF 12SLOT/10POLE MACHINE

Eccentricity type	Frequency order	Mode Order
Health	5,15,⋯	5,7,15,17⋯
SE	5,15,⋯	4,5,6,7,14,15,16,17⋯
DE	4,5,6,14,15,16⋯	4,5,6,7,14,15,16,17⋯
ME	4,5,6,14,15,16⋯	4,5,6,7,14,15,16,17⋯

Fig.3 shows the open-circuit flux-densities of the machine with SE, DE, and ME, separately captured at rotor position of 90 mech. degree with FEM method. As can be seen, the maximal flux density with eccentricity is always pointed to the minimum air gap while with SE, it is fixed but with DE and ME rotating. Fig.3 (b) reveals the spatial harmonics which are good agreement with analysis results. Among the 4th, 6th, 14th, 16th spatial harmonics brought by eccentricity, the amplitude of 6th is largest while the 4th mode order is lowest, these two should be paid particular attention.

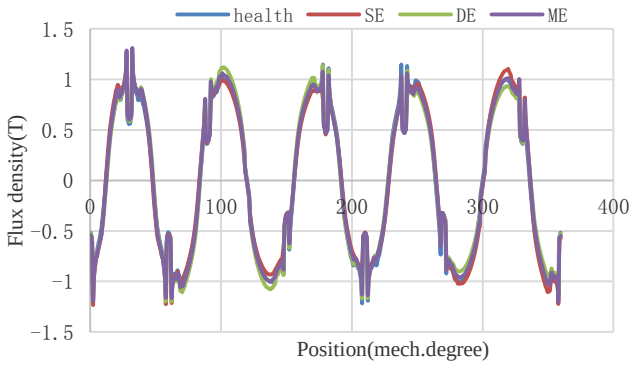

(a)

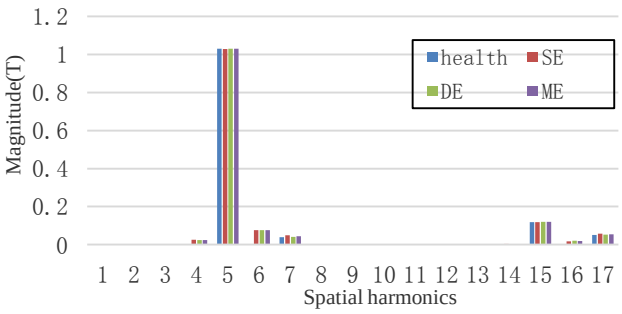

(b)

Fig.3 Radial component of open-circuit flux-densities on circular path away from stator bore by 0.15 mm with FEM. (a) waveforms. (b) Spectra, rotor position is 12 mech.degree.

B. Armature reaction field analysis

When the machine is with load, the field will contain not only magnet field but also armature reaction field. Similarly, the armature reaction field distribution can be achieved using the same method. In order to analyze conveniently, we assume a pure sinusoidal current in the windings, i.e., without considering the impact of the PWM modulation. The armature reaction field of health machine with load is:

$$\begin{aligned} B_{r\_arm} &= \sum_{m} B_m \cos[m\theta \pm (pw_r t + \theta_1)] \times \sum_{k_2}^{0,1,2} \Lambda_{k_2} \cos(k_2 N_s \theta) \\ &= \sum_{m} \sum_{k_2}^{0,1,2} B_m \Lambda_{k_2} \cos[(m \pm k_2 N_s)\theta \pm (pw_r t + \theta_1)] \\ m &= 3C \pm 1, C = 0, \pm 2, \pm 4, \cdots \end{aligned} \tag{11}$$

Where m is the order of the space harmonics; θ_1 is the phase current angles.

For three phase machines, the slot number must be a multiple of 3. So the armature reaction field frequency and spatial mode order can be described as:

$[\, pf_1, 3C \pm 1]$,

Where $C = 0, \pm 2, \pm 4, \cdots$

The armature reaction field distribution of eccentric machine can also be achieved by considering the modulation effect of non-uniform air-gap as in the open-circuit field.

SE:

$$\begin{aligned} B_{s\_r\_arm} &= \frac{B_{r\_arm}}{k_s} \\ &= \frac{\sum_{m} \sum_{k_2}^{0,1,2} B_m \Lambda_{k_2} \cos[(m \pm k_2 N_s)\theta \pm (pw_r t + \theta_1)]}{1 + \delta_s \cos(\theta - \theta_s)} \end{aligned} \tag{12}$$

DE:

$$\begin{aligned} B_{d\_r\_arm} &= \frac{B_{r\_arm}}{k_d} \\ &= \frac{\sum_{m} \sum_{k_2}^{0,1,2} B_m \Lambda_{k_2} \cos[(m \pm k_2 N_s)\theta \pm (pw_r t + \theta_1)]}{1 + \delta_d \cos(\omega_r t - (\theta - \theta_d))} \end{aligned} \tag{13}$$

ME:

$$\begin{aligned} B_{m\_r\_arm} &= \frac{B_{r\_arm}}{k_m} \\ &= \frac{\sum_{m} \sum_{k_2}^{0,1,2} B_m \Lambda_{k_2} \cos[(m \pm k_2 N_s)\theta \pm (pw_r t + \theta_1)]}{1 + \delta_s \cos(\theta - \theta_s) + \delta_d \cos(\omega_r t - (\theta - \theta_d))} \end{aligned} \tag{14}$$

For SE, the field frequency remains unchanged while the spatial mode order change while for DE and SE, both the corresponding frequency order and spatial mode order change and can be described as:

SE: $[\, p, 3C \pm 1]$,

DE: $[(\, p, p \pm 1), 3C \pm 1]$,

ME: $[(\, p, p \pm 1), 3C \pm 1]$,

where $C = 0, \pm 1, \pm 2, \cdots$

Fig.4 shows the armature reaction field flux-densities captured at rotor position of 90 mech. degree by FEM method. As can be seen, eccentricity brings 2th, 4th, 6th, 8th, etc. spatial harmonics. the amplitude of 4th is largest while the lowest mode order is 2th, these two should be paid particular attention.

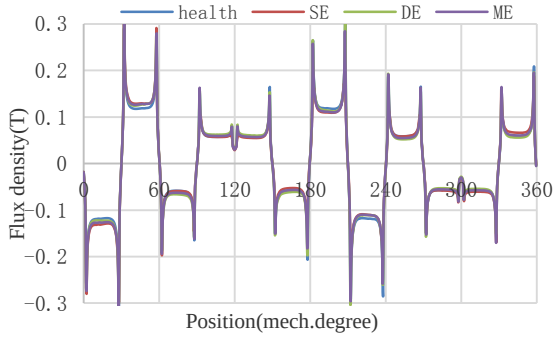

(a)

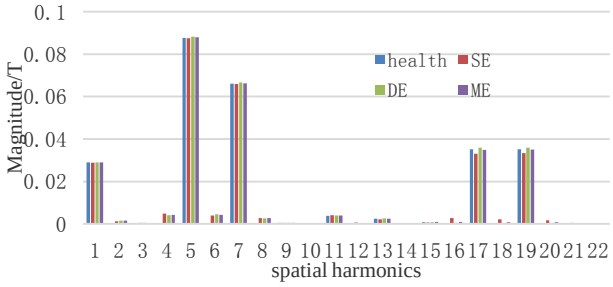

(b)

Fig.4 Radial component of armature reaction field flux-densities on circular path away from stator bore by 0.15 mm. (a) Waveforms (b) Spectra..

C. Load field analysis

When the machine is with load, using the superposition principle, the resultant air-gap flux density on load is given by [11]:

$$B_{r\_load} = B_{r\_mag} + B_{r\_arm} \quad (15)$$

From equation (7)-(10) and equation (11)-(14), we can get the spatial harmonic contents of PM machine. Fig.5 is the field distribution with load captured at rotor position of 90 mech. degree by FEM method. The spectra shown in Fig.5 (b) proves the validity of the superposition principle, hence the superposition principle will also be used in analyzing the mode order of the radial force.

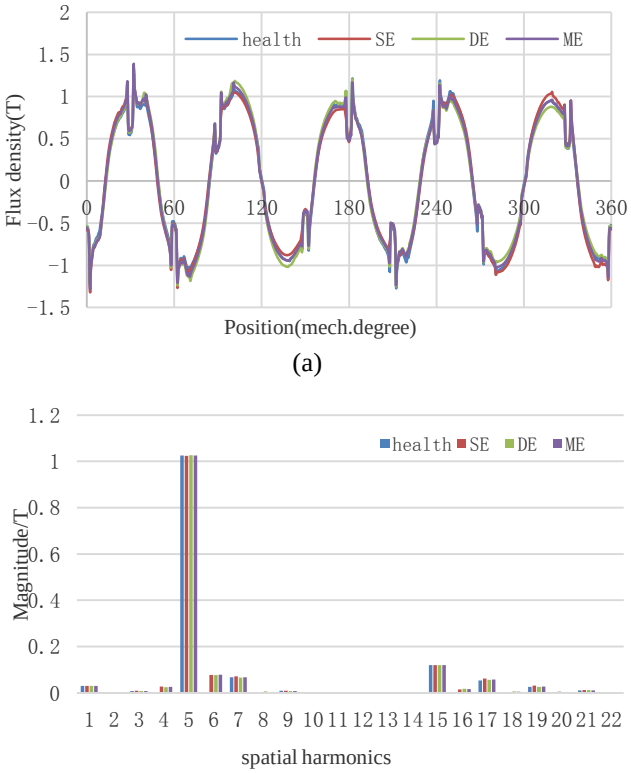

Fig.5 Radial component of load field flux-densities on circular path away from stator bore by 0.15 mm. (a) Waveforms (b) Spectra..

D. Cogging torque

Fig.6 compares the curve of cogging torque. From this figure, we can see that eccentricity will extremely enlarge the cogging torque. Table. II summarizes the P-P values of cogging torque. Cogging torque in DE situation is the largest because of the air-gap changes the most severe. Compared with other eccentricity, the influence of SE on cogging torque is slight.

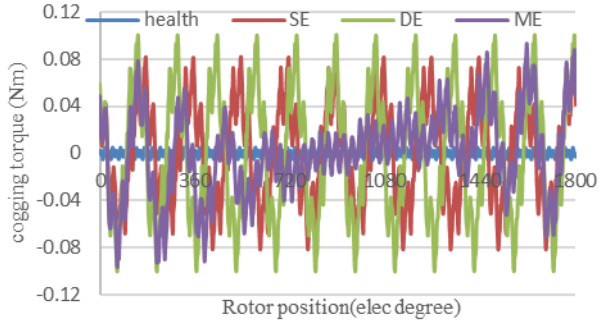

Fig.6 Cogging torque in a mechanical cycle

TABLE III. COGGING TORQUE OF THE SPM MOTOR

	health	SE	DE	ME
P-P values(mNm)	10.23	164.33	201.26	190.23

E. Back-EMF

Fig.7 shows the back-EMF of the motor. As can be seen form the figure, eccentricity has little effect on amplitude of back-EMF both in SE, DE and ME. A reasonable explanation is that for the coils of one phase, ones under the smaller air-gap induces a larger back-EMF while the ones under the larger air-gap induces a smaller back-EMF. Each phase remained almost the same after the compensation.

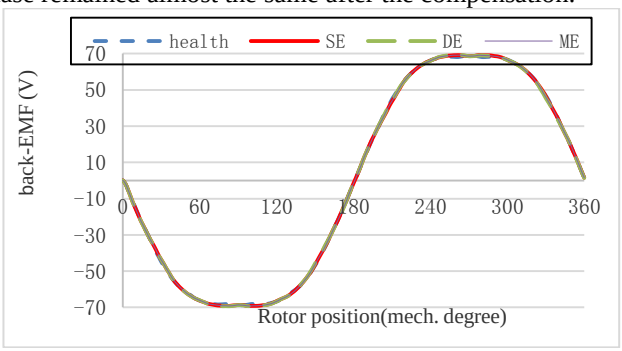

Fig.7 Back-EMF of motor under different eccentricity

F. Torque

Electromagnetic torque waveforms and their harmonics with different type of eccentricity are compared in Fig.8. Eccentricity almost has no influence on the average torque as shown in Table IV. The motor with DE exhibits the largest torque ripple (3.42%), which is about 0.228Nm, almost 3 SE on the torque ripple is smaller whose torque ripple is 0.175 Nm, nearly 2.3 times of the health. Because ME is a hybrid of SE and DE, Consequently, The effect of ME on torque ripple is smaller than DE and larger than SE.

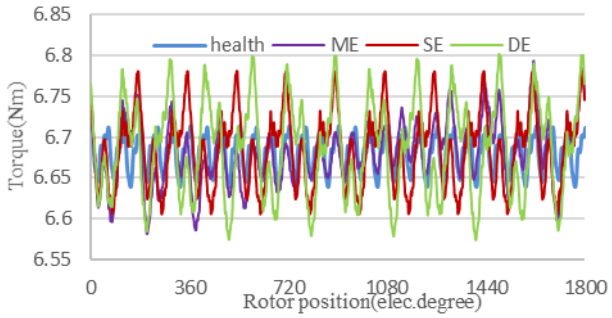

Fig.8 Comparison of electromagnetic torque in a mechanical cycle

TABLE IV. TORQUE OF THE SPM MOTOR

	health	SE	DE	ME
P-P values(Nm)	0.075	0.175	0.228	0.213
Average torque(Nm)	6.681	6.686	6.686	6.681
Torque ripple (%)	1.12	2.61	3.42	3.18

IV. UNBALANCED MAGNETIC PULL AND VIBRATION AND NOISE WITH ECCENTRICITY

A. *Radial Force distribution*

The radial force density in air region can be calculated by a simplified formula [11]:

$$F_r = \frac{B^2{}_{r\_load}}{2\mu_0} = \frac{(B_{r\_mag} + B_{r\_arm})^2}{2\mu_0} = \frac{B_{r\_mag}{}^2 + 2B_{r\_mag}B_{r\_arm} + B_{r\_arm}{}^2}{2\mu_0} \quad (16)$$

In[11], the author summarizes the three type spatial harmonic contents of radial force including: Assuming the spatial harmonic contents in the magnet field are $i_1, i_2, i_3, \cdots$, and those in reaction armature field are $i_1, i_2, i_3, \cdots$ respectively, then from the above formula, we can know that the radial force should include three components and their spatial harmonic are [11]:

(a) $k = 2i_u$ and $i_u \pm i_v$ $u = v = 1,2,3\cdots$ Caused by the magnet field only (i.e. open circuit field);

(b) Caused by the armature reaction field only;

(c) Caused by the magnet field and the armature reaction field.

Combined equation (7)-(10) with equation (11)-(14), we can get the spatial harmonic contents of PM machine. Those of investigated 12slot/10pole machine are summarized in Table V. The radial force spatial harmonic contents of eccentric machine have greatly expanded both for no load and with load condition. For example, in static eccentricity for open-circuit, the 1th, 3th, 8th, 9th, 11th …occur besides the 2th, 10th, 12th ⋯ already exist in health machine. For load condition, the harmonic contents also broaden and odd harmonics began to emerge. In addition, for different types of eccentricity, the spatial harmonic contents are the same but with various amplitude.

Fig.9 and Fig.10 show the radial force with FEM method without load and with load, separately. As can be seen from the figure, the calculated results are in completely accord with theoretical analysis shown in Table V, this proves the correctness of the theoretical analysis.

TABLE V. SPATIAL HARMONIC ORDER OF RADIAL FORCE

	Interaction by magnet field only	Interaction by armature reaction field only	Interaction between magnet field and armature reaction field
Health	2,10,12 …	2,4,6,8,10,12,14, …	2,4,6,8,10,12,14,16,⋯
SE	1,2,3,8,9,10,11,12, …	1,2,3,4,5,6,7,8,9, 10,11,12,13⋯	1,2,3,4,5,6,7,8,9,10,11, 12,13,14,15,16,⋯
DE	1,2,3,8,9,10,11,12, …	1,2,3,4,5,6,7,8,9, 10,11,12,13⋯	1,2,3,4,5,6,7,8,9,10,11, 12,13,14,15,16,⋯
ME	1,2,3,8,9,10,11,12, …	1,2,3,4,5,6,7,8,9, 10,11,12,13⋯	1,2,3,4,5,6,7,8,9,10,11, 12,13,14,15,16,⋯

TABLE VI. FREQUENCY ORDER OF RADIAL FORCE

	Interaction by magnet field only	Interaction by armature reaction field only	Interaction between magnet field and armature reaction field
Health	10,20,30,40, ⋯	2,4,6,8,10,12,14, …	2,4,6,8,10,12,14,16,⋯
SE	10,20,30,40, ⋯	1,2,3,4,5,6,7,8,9, 10,11,12,13⋯	1,2,3,4,5,6,7,8,9,10,11, 12,13,14,15,16,⋯
DE	1,2,3,8,9,10,11,12, …	1,2,3,4,5,6,7,8,9, 10,11,12,13⋯	1,2,3,4,5,6,7,8,9,10,11, 12,13,14,15,16,⋯
ME	1,2,3,8,9,10,11,12, …	1,2,3,4,5,6,7,8,9, 10,11,12,13⋯	1,2,3,4,5,6,7,8,9,10,11, 12,13,14,15,16,⋯

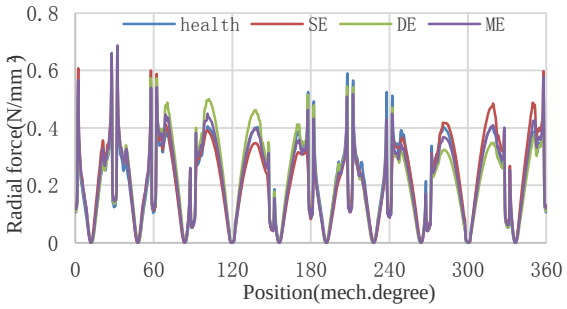

(a)

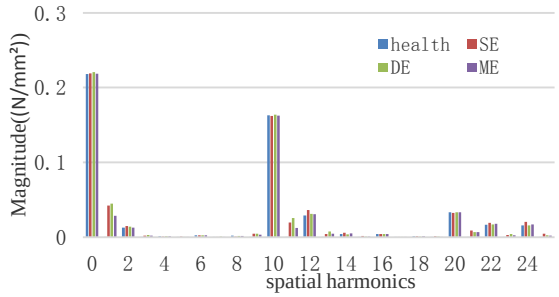

(b)

Fig.9 Radial force on circular path away from stator bore by 0.15 mm for no load condition. (a) Waveforms (b) Spectra..

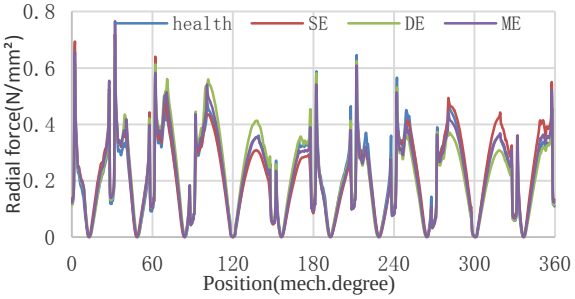

(a)

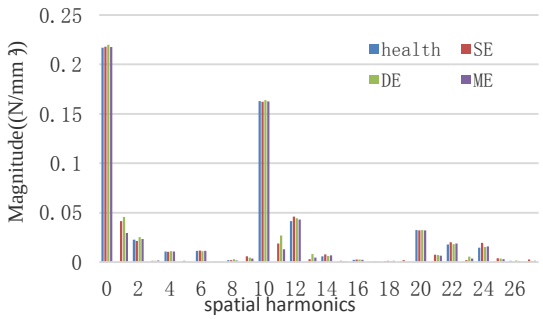

(b)

Fig.10 Radial force on circular path away from stator bore by 0.15 mm with load. (a) Waveforms (b) Spectra.

The radial force distribution of health machine is time-independent. However, it is not so when eccentricity exists. Fig. 11 shows the radial force distribution of SE and DE with load condition. The force distribution of SE is always towards the small air-gap while the DE is rotates with the small air-gap. This is also true for no load condition.

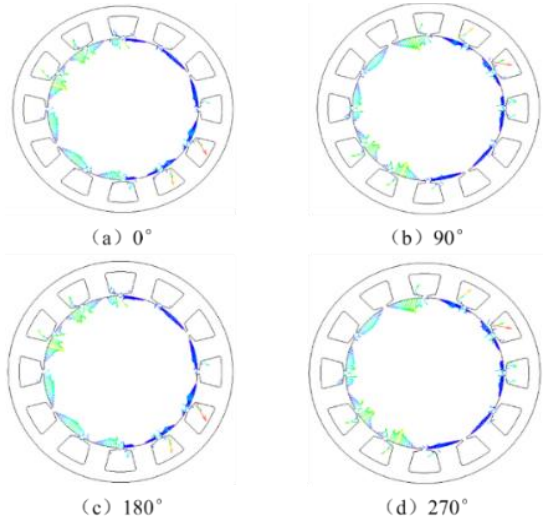

(a) SE motor

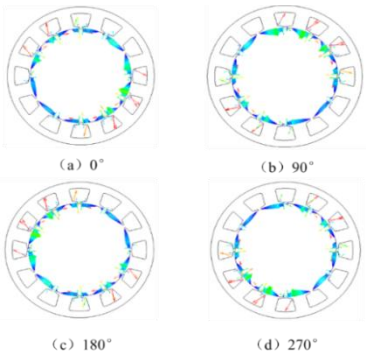

(b) DE motor

Fig.11 The radial force distribution with rated load

B. Unbalanced magnetic pull(UMP)

Eccentricity always brings unbalanced magnetic pull (UMP). Fig.12 compares the change of unbalanced magnetic pull. The health 12slot/10pole machine doesn't have UMP. Comparing Fig.12 (a) and (b), we can find that the UMP is almost unrelated to the load condition of motor. Besides, we can discover a phenomenon that the cycle of UMP are obvious in SE and DE. In SE, the cycle is 10 in a mechanical cycle, namely, the number of rotor pole. In DE, it is 12, the number of stator tooth. But in ME, the cycle is complicated, it is difficult to estimate the cycle.

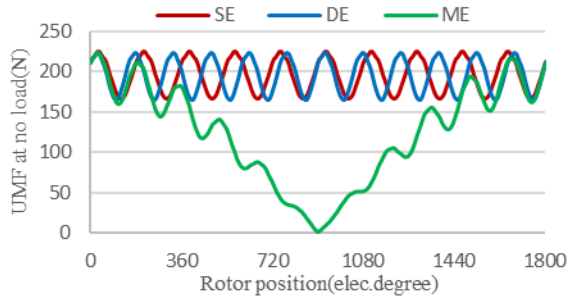

(a) no load

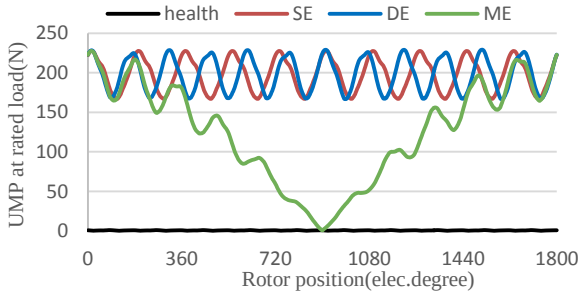

(b) full load

Fig.12 Comparison of UMP waveforms without/with load

Fig.13 shows the variation of UMP direction with load. The UMP direction in SE condition is nearly fixed towards the smallest air-gap. Thus, the rotor is attracted by the stator and will accelerate the bearing wearing, the wearing of bearing will further increase the degree of the SE. As a result, a positive feedback is formed, the life of the motor with SE will be shortened. In DE condition, the UMP direction rotates with the minimum air-gap. In ME condition, the direction is determined by the ratio of SE and DE. For no load condition, this will be similar only the difference of the amplitude.

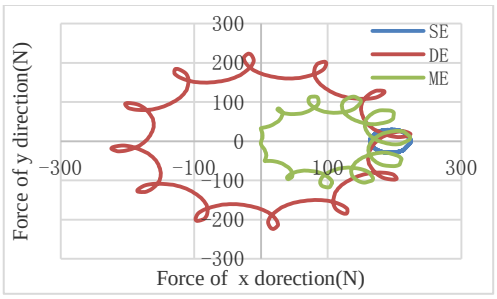

Fig.13 Comparison of the UMP direction with load

D. *Modes analysis*

Modes analysis is a priority for the study of motor vibration. In this paper, the 3D-FEA structure analysis of JMAG software is applied to calculate the natural frequencies of vibration mode. The materials are set as follows: the Yong's module and Poisson's ratio of lamination are set to 2×10^{11} Pa and 0.3, respectively. The aluminum house are set to 6.9×10^{10}Pa and 0.33, respectively. For the windings, their weight is treated as an extra weight in the stator and distributed over the effective lamination, reference to[15].The end-caps are fixed on the house which are assumed to be perfectly contacted with the house while the house is fixed on the mounting plate of test rig by the bolts, as shown in Fig.14 (a). In the FEA analysis, we assume that the rotor is treated as concentrated mass and neglect the influence of bearing and the stiffness of winding.

Fig.14 (b), (c) and (d) shows the radial mode 1, 2, 3 of the motor respectively, the aluminum house and end-caps are hidden in order to show more clearly. Their natural frequencies in the range of 7000 Hz are summarized in Table VI.

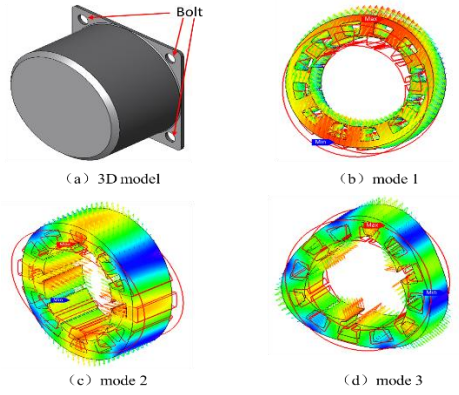

Fig.14 Vibration modes of the motor (a) health model; (b) mode 1; (c) mode 2; (d) mode 3

TABLE VII. NATURAI FREQUENCY OF THE STATOR PART

	Natural frequencies(Hz)
Mode 1	608.6, 610.1, 1718,1721, 2682, 2689, 4504, 5504, 5523,
Mode 2	3225, 3327, 3936
Mode 3	5119, 5150

E. *Vibration and noise*

Fig.15 shows the motor vibration spectra of the stator house with/without load conditions at frequency of 0~6000 Hz. The vibration with eccentricity has greatly changed compared with health machine no matter with or without load. Fig.16 reveals the vibration distribution in the natural frequency of 1718 Hz. The resonance vibration of health machine is usually small due to the radial force doesn't exist in natural frequency, while the eccentric machines will be enormously excited because of the additional specific radial force which frequency and spatial mode order are satisfied to the inherent frequency of stator vibration modes. Besides the mode 1 natural frequency, in the natural frequency of 5119 Hz which vibration mode is 3, the maximal vibration of SE, DE, ME are 81, 194, 104 m/s^2 while the health machine is only 1m/s^2.In the eccentric machines different types of eccentricity exhibit various vibration amplitude in natural frequencies which are caused by different amplitude force. In conclusion, the eccentricity increases not only vibration amplitude at certain frequency, but also increase the content of vibration frequency of the motor.

As the consequence of vibration, the acoustic noise is predicted and compared in Fig.17. The noise is calculated 200 mm away from the motor house. From the figure, we can find that the eccentricity will slightly increase the noise level of the machine at no load condition but the noise level will greatly increase if the motor with load.

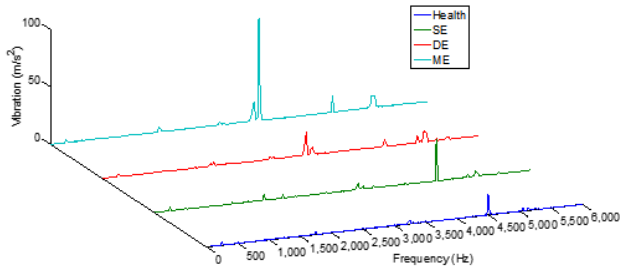

(a) no load

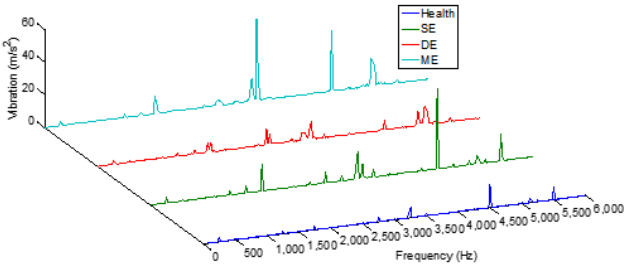

(b) full load

Fig.15 Comparison of vibration of the motor house at 1500 rpm

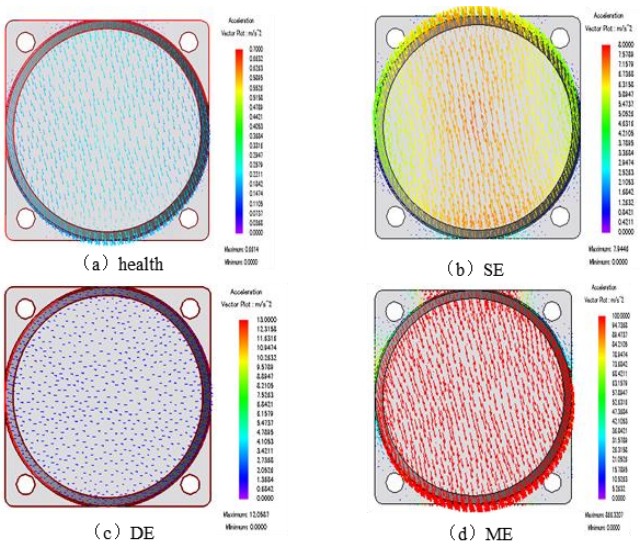

Fig.16 Vibration distributionof the motor house of 1718Hz in 1500 rpm

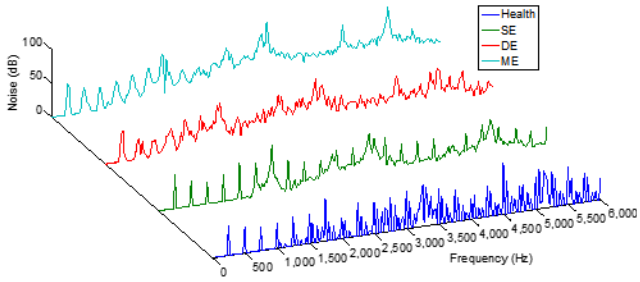

(a) no load

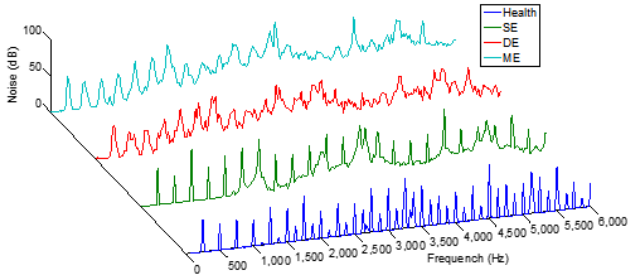

(b) full load

Fig.17 Comparison of acoustic noise of motor at 1500 rpm

V. EXPERIMENTAL VERIFICATION

A. *Experiment set-up*

The experiment set-up is shown in Fig.18. The vibration sensor and data collector is the B&K company product which model are 4514-B-001 and 3050-B-040, the tested machine is driven by special servo controller using speed control mode, the magnetic powder dynamometer can adjust the load torque by current. It is very regrettable that there are no eccentric machine and we can only measure the vibration of health machine. Besides, due to the noise interference come from the controller of the magnetic powder dynamometer which is very close from the tested motor, so we don't measure the noise neither.

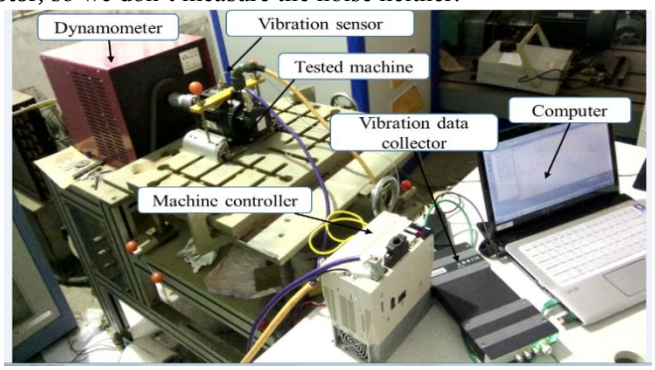

Fig.18 Experimental setup

B. *Measurement results*

Fig. 19 displays the measured health machine vibration results with/without load which are not well agreed with the calculated results. The reasonable explanation may be two aspects: One is in 3D structure analysis, we don't consider the actual radiating rib on house which may have an inhibition effect on vibration. The other may be the mesh quality is poor because of the large memory consumption of 3D FEM. Nevertheless, the variation trend is acceptable and proves the rationality of the theoretical analysis

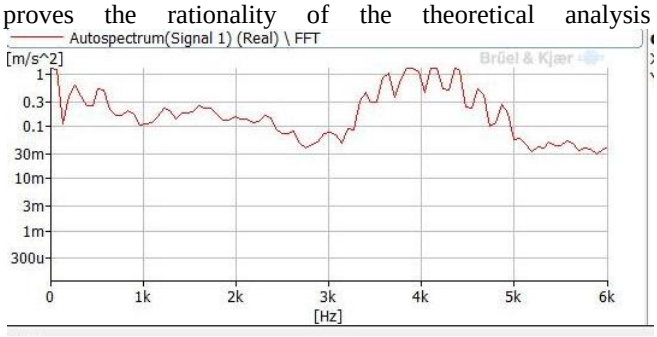

(a) No load

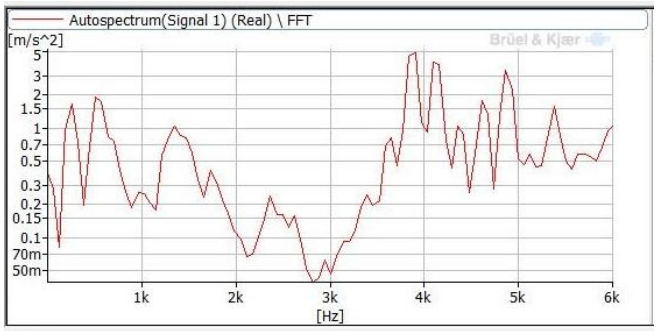

(b) With load

Fig.19 Measured vibration spectra for health machine at 1500 rpm

VI. CONCLUSIONS

The performance of an SPM servo motor with SE, DE

and ME eccentricity is analyzed and compared especially for radial force and vibration and noise. It is found that the frequency and mode order of radial force extend for eccentric machine. Different types of eccentricity have various influence on the radial force. For example, the SE only change the mode order of radial force while DE and ME expand both the frequency spectra and mode order. As the result of eccentricity, vibration and noise tremendously increase for eccentric machine in virtue of the radial force frequency of eccentric machines is more easer to close to the natural frequency and force mode coincide with the machine mode, thus, a large vibration will generate, as a consequence, the noise also increases obviously.

REFERENCES

[1] Sang-Moon Hwang, Kyung-Tae Kim, "Comparison of Vibration Sources Between Symmetric and Asymmetric HDD Spindle Motors With Rotor Eccentricity," *IEEE Trans. Ind.Appl*, vol. 37, no. 6, pp. 1727–1531, Nov.2001,

[2] Jian Li, Dawoon Choi and Yunhyun Cho, "Analysis of Rotor Eccentricity in Switched Reluctance Motor with Parallel Winding Using FEM," *IEEE Trans. Magnetics* , vol. 45,no.6, pp. 2851–2854, June,2009.

[3] X.Liu, Z.Q.Zhu and M,Hasegawa "Vibration and Noise in Variable Flux Reluctance Machine With DC-Field Coil in Stator," in *IPEMDC-ECCE Asia.*. Harbin, China, pp. 1100–1107, June. 2012.

[4] Z. Q. Zhu, L. J. Wu, and M. L. Mohd, "Distortion of Back-EMF and Torque of PM Brushless Machines Due to Eccentricity," *IEEE Trans. Magnetics* , vol. 49,no.8, pp. 4927–4935, August,2013.

[5] Min-Fu. Hsieh and Yu-Han. Yeh. "Rotor Eccentricity Effect on Cogging Torque of PM Generators for Small Wind Turbines," *IEEE Trans. Magnetics*, vol. 49,no. 5, pp. 1897–1900, MAY,2013.

[6] Bashir Mahdi Ebrahimi, Jawad Faiz and Mehrsan Javan Roshtkhari. "Static-, Dynamic-, and Mixed-Eccentricity Fault Diagnoses in Permanent-Magnet Synchronous Motors," *IEEE Trans. Industrial Electronics*, vol. 56,no. 11, pp. 1897–1900, Nov,2009.

[7] R.O. Duda, P. E. Hart, and D. G. Stork, *Pattern Classification, 2nd ed.* New York:Wiley, 2002

[8] G. Niu, J. D. Son, A. Widodo, B. S. Yang, D. H. Hwang, and D. S. Kang, "A comparison of classifier performance for fault diagnosis of induction motor using multi-type signals," *Struct. Health Monit.* vol. 6, no. 3, pp. 215–229, 2007.

[9] Y. S. Chen, Z. Q. Zhu, and D. Howe, "Vibration of PM Brushless Machines Having a Fractional Number of Slots Per Pole," *IEEE Trans. Magnetics*, vol. 42, no. 10, pp. 3395–3397, Oct,2006

[10] S. Huang, M. Aydin, T. A. Lipo,"Electromagnetic Vibration and Noise Assessment for Surface Mounted PM Machines," *IEEE*, 2001.

[11] Z. Q. Zhu, Z. P. Xia, L. j. Wu, and G. W. Jewell," Influence of Slot and Pole Number Combination on Radial Force and Vibration Modes in Fractional Slot PM Brushless Machines Having Single- and Double-layer Windings," *IEEE*, 2009.

[12] Z. Q. Zhu, Z.P. Xia, L. J. Wu, and G.W. Jewell, "Analytical modelling and finite element computation of radial vibration force in fractional-slot permanent magnet brushless machines," IEEE International Electric Machines and Drives Conference, *IEMDC2009, Florida USA*, May 3-6, 2009, pp.157-164.

[13] Z. Q. Zhu, Howe D, "Instantaneous magnetic field distribution in brushless permanent magnet do motors, Part III: Effect of stator slotting," *IEEE Transactions on Magnetics*, 1993, vol. 29, no. 1, pp.143 — 151,1993

[14] H. D. Yang, "Electromagnetic Vibration Analysis of Permanent Magnet Synchronous Motor," [D.Sc. (Tech.) Thesis]. China; Zhejiang University, 2011

[15] S.A. Long, Z. Q. Zhu, and D. Howe, "Vibration behaviour of stators of switched reluctance motors," *IEEE Proc. Electr. Power Appl.*, vol.148, no.3, pp.257-264, May 2001